# Heat Transfer and Pressure Drop of a Supercritical Pressure Fluid Flowing in a Tube of Small Diameter

Yamashita, Tohru
Department of Mechanical Engineering Science : Graduate Student

Mori, Hideo
Department of Mechanical Engineering Science : Associate Professor

Yoshida, Suguru
Faculty of Engineering, Kyushu University : Professor Emeritus

Ohno, Masaki
Faculty of Engineering, Kyushu University : Researcher

https://hdl.handle.net/2324/3315

出版情報：九州大学工学紀要. 63 (4), pp.227-244, 2003-12. 九州大学大学院工学研究院
バージョン：
権利関係：

Memoirs of the Faculty of Engineering, Kyushu University, Vol. 63, No. 4, December 2003

# Heat Transfer and Pressure Drop of a Supercritical Pressure Fluid Flowing in a Tube of Small Diameter

by

Tohru YAMASHITA,* Hideo MORI,** Suguru YOSHIDA*** and Masaki OHNO†

(Received September 24, 2003)

**Abstract**

In relation to the development of a Supercritical pressure water Cooled Power Reactor (SCPR), experiments were performed on heat transfer and pressure drop of a supercritical pressure fluid flowing upward in a uniformly heated vertical smooth tube of a small diameter 4.4 mm, using HCFC22 as a test fluid.

Characteristics of the heat transfer were clarified for the small diameter tube, comparing with the data obtained previously with tubes of large diameter. General characteristics of the heat transfer were found to be similar to those in the tubes of large diameter. The effect of the tube diameter on the heat transfer was seen for a 'normal' heat transfer, but not for a 'deteriorated' heat transfer. The limit heat flux for the occurrence of deterioration in heat transfer becomes larger with the tube of smaller diameter. For the 'normal' heat transfer, the Watts and Chou correlation showed the best predicting performance.

Frictional pressure drop becomes smaller than that for an isothermal flow in the region near the pseudocritical point, and this reduction was more remarkable in the 'deteriorated' heat transfer.

**Keywords:** Supercritical pressure fluid, Heat transfer, Pressure drop, Flow in small diameter tube, Vertically upward flow

## 1. Introduction

Recently the development of a Supercritical pressure water Cooled Power Reactor (SCPR) as an advanced nuclear power reactor proceeds in relation to a high attention to environmental problems. The SCPR is a once-through type water cooled nuclear reactor supplying high temperature supercritical pressure steam to the turbine system and is expected to achieve higher plant efficiency and a simpler plant system than current nuclear power plants[1]. In the design of the SCPR core, thermohydraulic characteristics, that is, characteristics of heat

*Graduate Student, Department of Mechanical Engineering Science
**Associate Professor, Department of Mechanical Engineering Science
***Professor Emeritus, Faculty of Engineering, Kyushu University
†Researcher, Faculty of Engineering, Kyushu University

transfer and pressure drop of supercritical pressure fluids are important for the performance and safety.

It is well known that, when liquid is heated at a constant supercritical pressure, there is no phase change at a constant temperature, and there is a continuous variation from a liquid-like fluid to a vapor-like fluid. Therefore, supercritical pressure fluids in a thermodynamic equilibrium state can be regarded as single phase fluids in any conditions from a macroscopic standpoint. Their physical properties, however, vary rapidly with temperature as the example shown in **Fig. 1**. At a vicinity of the pseudocritical temperature $T_{pc}$ which is defined as the temperature with a peak of the specific heat at constant pressure $c_p$, physical properties such as thermal conductivity $\lambda$, density $\rho$, viscosity $\mu$ and specific enthalpy $h$ vary rapidly from liquid-like state to vapor-like state. Heat transfer and pressure drop of the supercritical pressure fluid are characterized by such variations of physical properties with temperature.

On the development of supercritical pressure fossil power plant boilers, many investigations on the heat transfer to supercritical pressure fluids have been made mainly with the tubes of diameter over 10 mm using water or carbon dioxide as the test fluid[2-7]. From these investigations, it has been found that the heat transfer to supercritical pressure fluids has two characteristics; a 'normal' heat transfer at a low heat flux and a 'deteriorated' heat transfer at a high heat flux.

In the 'normal' heat transfer, the heat transfer coefficient has a peak near the pseudocritical point, and this peak reduces as the heat flux increases. This characteristic was explained by the radial variations of the physical properties near the wall with the temperature. Therefore, a single phase heat transfer correlation for a constant property fluid such as the well-known Dittus and Boelter correlation[8] is no longer applicable to the supercritical pressure fluid. Various heat transfer correlations have been proposed for the 'normal' heat transfer based on experimental data for water and/or carbon dioxide. Most of these correlations are expressed in the form of a constant properties heat transfer correlation equation multiplied by the ratios of properties between the bulk fluid temperature and the wall

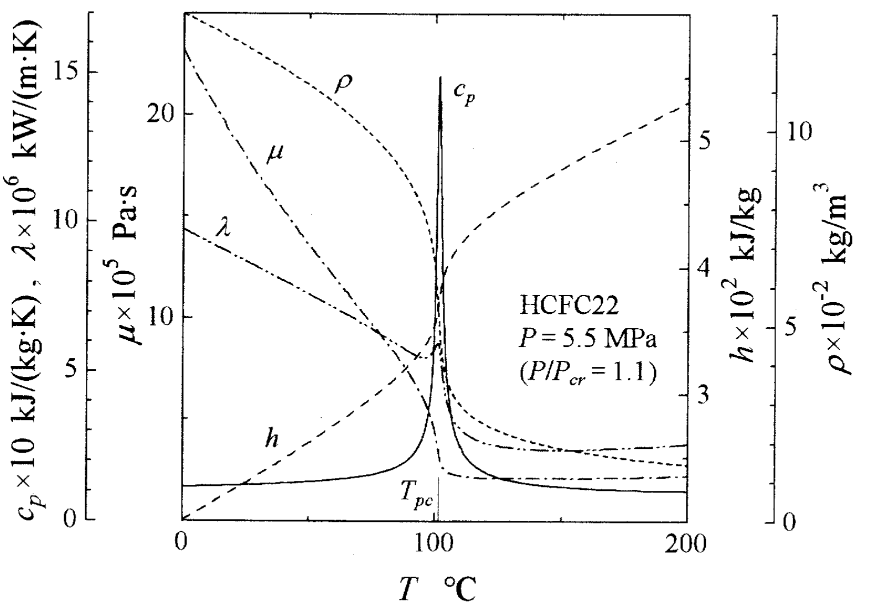


**Fig. 1** Physical properties of HCFC22 at a supercritical pressure

temperature.

In the 'deteriorated' heat transfer, the heat transfer becomes worse where the bulk fluid enthalpy is below the enthalpy of the pseudocritical point. For water, Yamagata *et al.*[6] proposed the empirical equation for the limit heat flux above which the deterioration in heat transfer occurs. In respect to the heat transfer deterioration, Jackson and Hall[7] obtained the criterion for negligible buoyancy effects for the upward flow in the vertical tube. Further, Yoshida *et al.*[9,10] have obtained the criterion for the occurrence of deterioration in heat transfer based on the data for freons experimentally.

For the pressure drop of supercritical pressure fluids flowing in tubes, there are a few investigations. Ishigai *et al.*[11] have obtained the empirical friction factor correlation for the 'normal' heat transfer, based on the experimental data of frictional pressure drop of supercritical pressure water flowing in uniformly heated tubes.

In the Supercritical pressure water Cooled Power Reactor (SCPR) core, a tightened fuel rod pitch of which a hydraulic diameter is 4.4 mm will be adopted. There are, however, only a few experimental data on the heat transfer and few data on the pressure drop for supercritical pressure fluids in tubes of such a small hydraulic diameter[11-13]. Especially on the pressure drop, very few studies have been made so far, including the case for the large diameter tube.

In the present study, experiments were performed on the heat transfer and pressure drop of a supercritical pressure fluid flowing vertically upward in a uniformly heated smooth tube having a small diameter of 4.4 mm, using HCFC22 as the test fluid. The heat transfer characteristics for the small diameter tube were clarified, and the effects of tube diameter on the heat transfer were also made clear, comparing with the data having been obtained with tubes of larger diameter[9,14]. For the 'normal' heat transfer, the predicting performance of the correlations proposed by several researchers was tested. In addition, the frictional pressure drop was evaluated from the measured total pressure drop and its characteristics were examined in the relation with the heat transfer.

## 2. Experimental Apparatus and Methods

The experimental apparatus was a forced circulation test loop for freons as shown schematically in **Fig. 2**. HCFC22 was used as the test fluid. Its critical pressure and temperature, 4.99 MPa and 96.2 ℃, are much lower than those of water, 22.1 MPa and 373.9 ℃. HCFC22 is, therefore, suitable for use in the experiment to obtain the accurate and systematic data on the heat transfer and pressure drop at a supercritical pressure.

HCFC22 leaving the circulation pump was heated up to the required temperature through the preheater and led to the test section. HCFC22 leaving the test section was cooled through the cooler and returned to the circulation pump. The pressure in the loop was kept constant by an accumulator connected to a high pressure nitrogen gas supply. The flow rate and the pressure of HCFC22 were measured with a Coriolis type flow meter and a Bourdon-tube pressure gauge, respectively, at the inlet of the test section. The bypass loop was built in, to keep the stable flow in the test section.

The test section was an Inconel 600 smooth tube of 4.4 mm I.D. and 6.4 mm O.D. oriented vertically, as shown schematically in **Fig. 3**. It was heated over a 2 m length by passing alternating current through the tube directly. HCFC22 flows through the test section vertically upward. The inlet and outlet bulk fluid temperatures were measured with sheath thermocouples at the inlet and outlet mixing chambers, and the wall temperatures of the tube outside surface were measured with sheath thermocouples fixed at axially 50

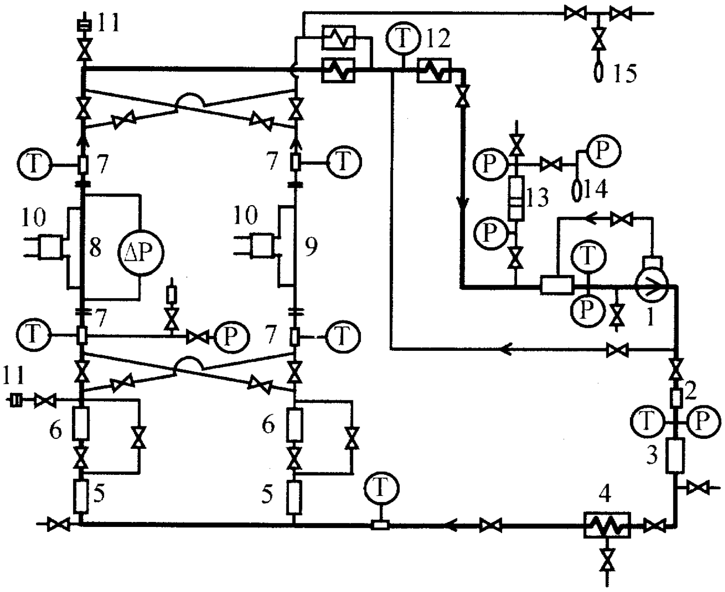

| | | | |
|---|---|---|---|
| 1 | Circulation pump | 11 | Blow-out disc |
| 2 | Filter | 12 | Cooler |
| 3 | Flow meter (orifice type) | 13 | Accumulator |
| 4 | Preheater | 14 | Nitrogen supply |
| 5 | Flow meter (coriolis type) | 15 | Freon supply |
| 6 | Flow control valve | (T) | Sheath thermocouple |
| 7 | Mixing chamber | (P) | Pressure gauge |
| 8 | Test section | (ΔP) | Differential pressure transmitter |
| 9 | Bypass section | | |
| 10 | Power supply | | |

**Fig. 2** Experimental apparatus

mm intervals, in total 39 sections. The fluid pressure difference or drop from the inlet to the outlet of the heated section was measured with the differential pressure transmitter connected at the inlet and outlet pressure taps.

In the experiments, keeping the constant pressure, flow rate, inlet fluid enthalpy and heat flux, the data were taken after confirming the wall temperatures at steady. The inside surface temperatures of the tube were evaluated from the measured outside surface temperatures taking account of the radial heat conduction within the tube wall. The bulk fluid temperature at each axial section corresponding to the position of measuring the outside surface temperature was evaluated from the bulk fluid enthalpy determined by the measured inlet fluid enthalpy and the heat balance from the test section inlet.

The heat transfer coefficient $\alpha$ was calculated from the inside surface heat flux $q$ and the temperature difference $T_w - T_b$ between the inside surface and the bulk fluid.

$$\alpha = \frac{q}{T_w - T_b} \quad (1)$$

The accuracy of the heat transfer coefficient was within about ±10%, although up to ±30% at the near-pseudocritical point at which the heat transfer coefficient has a peak at a low heat flux. The tube wall temperature was kept under 160 °C to avoid the deposition of carbon onto the wall surface due to the decomposition of HCFC22.

The experimental conditions are listed in **Table 1**. The pressure of 5.5 MPa corresponds to the reduced pressure, that is, the ratio of the pressure to the critical pressure $P/P_{cr}$ of 1.1,

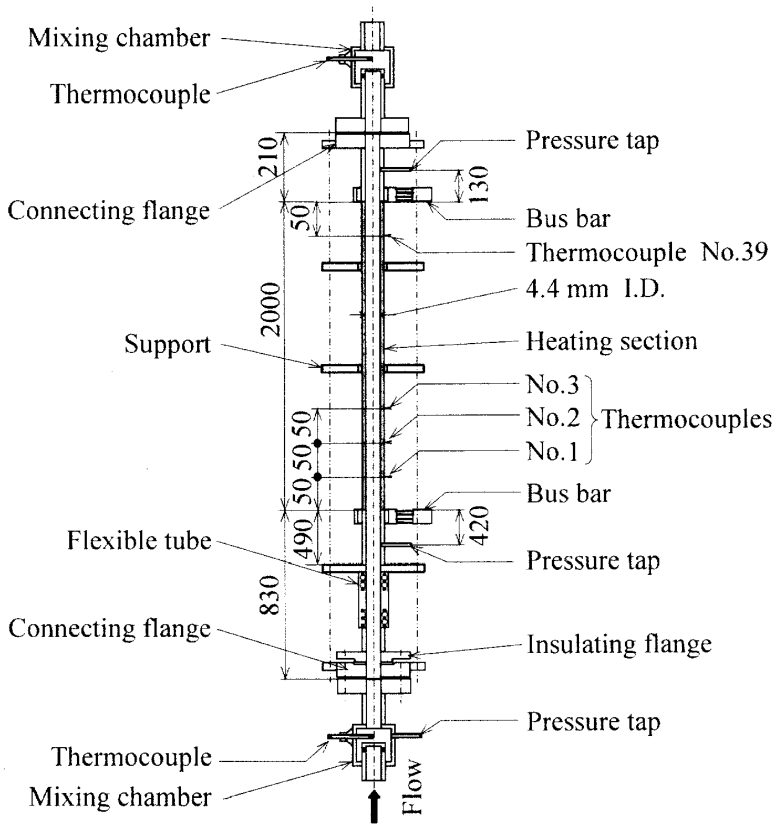


**Fig. 3** Test section

which is the same as the supercritical pressure water condition in the SCPR. Experiments for the heat transfer were made at various mass velocities of 400 to 2000 kg/(m$^2$·s), while experiments for the pressure drop were at 700 kg/(m$^2$·s). The physical properties of HCFC22 were calculated by NIST REFPROP Ver.6.0[15]. At 5.5 MPa, the pseudocritical temperature $T_{pc}$ and pseudocritical enthalpy $h_{pc}$ are 101.4 °C and 372.9 kJ/kg, respectively.

**Table 1** Experimental conditions

| | |
|---|---|
| Fluid | HCFC22 |
| Flow direction | Vertically upward |
| Inside diameter $D$ mm | 4.4 |
| Pressure $P$ MPa ($P/P_{cr}$) | 5.5 (1.1) |
| For heat transfer experiment | |
| Mass velocity $G$ kg/(m$^2$·s) | 400, 700, 1000, 1500, 2000 |
| Heat flux $q$ kW/m$^2$ | 10-170 |
| Bulk fluid enthalpy $h_b$ kJ/kg | 215-360 |
| For pressure drop experiment | |
| Mass velocity $G$ kg/(m$^2$·s) | 700 |
| Heat flux $q$ kW/m$^2$ | 0-60 |
| Bulk fluid enthalpy $h_b$ kJ/kg | 225-395 |

## 3. Experimental Results and Discussions

### 3.1 Characteristics of Heat Transfer

#### 3.1.1 General heat transfer characteristics

The measured inside surface temperatures of the tube wall $T_w$ and heat transfer coefficients $\alpha$ at the mass velocity of 400 and 1000 kg/(m$^2$·s) are plotted against the bulk fluid enthalpy $h_b$ in **Figs. 4 and 5**, respectively, with the heat flux $q$ as a parameter. In each diagram, solid symbols denote the axially first measuring positions for the data obtained at different inlet enthalpies. The heat transfer coefficient calculated by the Dittus and Boelter correlation[8] is also shown in the lower diagram of each figure.

From these figures, it was found that characteristics of the heat transfer in the small diameter tube are similar to those in larger diameter tubes.

At low heat fluxes, the following characteristic of the 'normal' heat transfer was seen. The wall temperature increases gradually with increasing the bulk fluid enthalpy, and the heat transfer coefficient has a peak when the bulk fluid enthalpy is slightly lower than the pseudocritical enthalpy $h_{pc}$. This peak becomes lower as the heat flux increases.

At higher heat fluxes, however, the wall temperature excursion, that is, the deterioration in heat transfer was observed. Two different types of temperature excursion can be recognized on the wall temperature distributions: One is a broad peak that extends over a wide

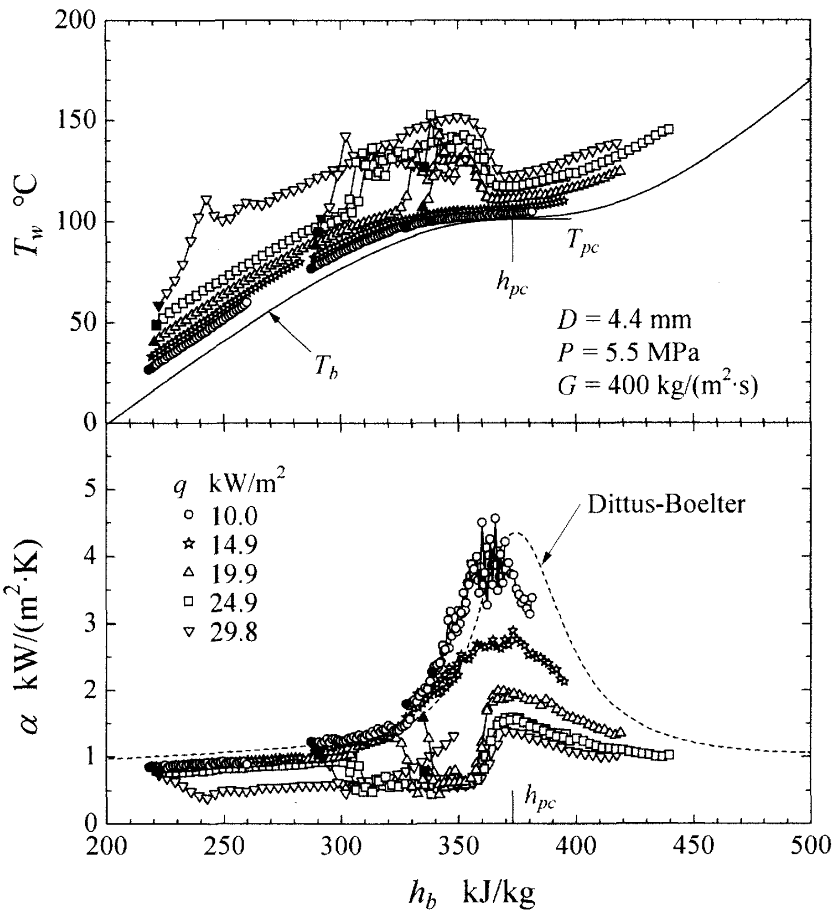


**Fig. 4** Relations of wall temperature and heat transfer coefficient with bulk fluid enthalpy at low mass velocity

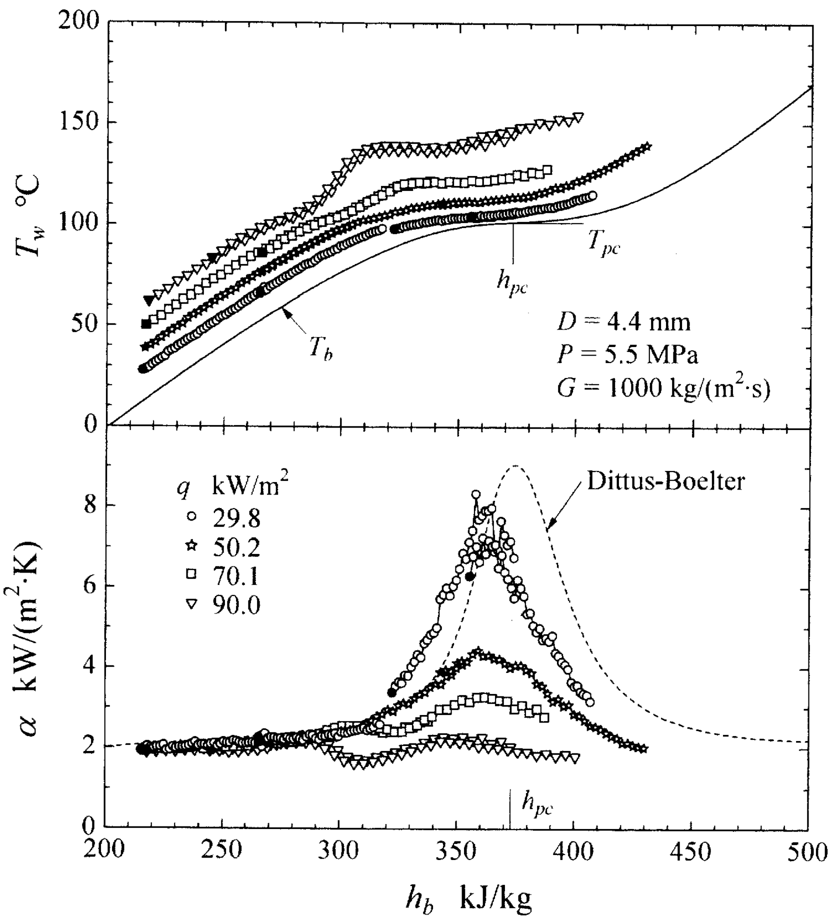


**Fig. 5** Relations of wall temperature and heat transfer coefficient with bulk fluid enthalpy at high mass velocity

range of bulk fluid enthalpy below the pseudocritical point, and the other is a sharp peak that is much more localized at a low flow rate. The first type of deterioration is considered to be an extension of the trend in the 'normal' heat transfer, that is, with increasing heat flux, the peaking of the heat transfer coefficient is suppressed and the heat transfer coefficient in the pseudocritical region becomes lower than that in the liquid region far away from the pseudocritical point. The second type of deterioration is considered to be caused by the modification on shear stress distribution across the tube due to buoyancy in low density layer near the wall, with consequential less production of turbulence[7].

### 3.1.2 Effects of tube diameter on the heat transfer

**Figure 6** illustrates the comparison of the measured heat transfer coefficients $\alpha$ with the data obtained previously with the tubes of larger diameter 9 and 13 mm for HCFC22[9,14], in the relation between the heat transfer coefficient and the bulk fluid enthalpy. In each diagram, the heat transfer coefficient calculated by the Dittus and Boelter correlation is also shown.

In the 'normal' heat transfer as shown in **Fig. 6(a)**, the heat transfer coefficient becomes larger with the smaller diameter tube. The similar effect of the tube diameter can be also seen in **Fig. 6(b)**, in the region of the enthalpy up to 310 kJ/kg at which the deterioration in heat transfer occurred. The degree of the increase in the heat transfer coefficient with

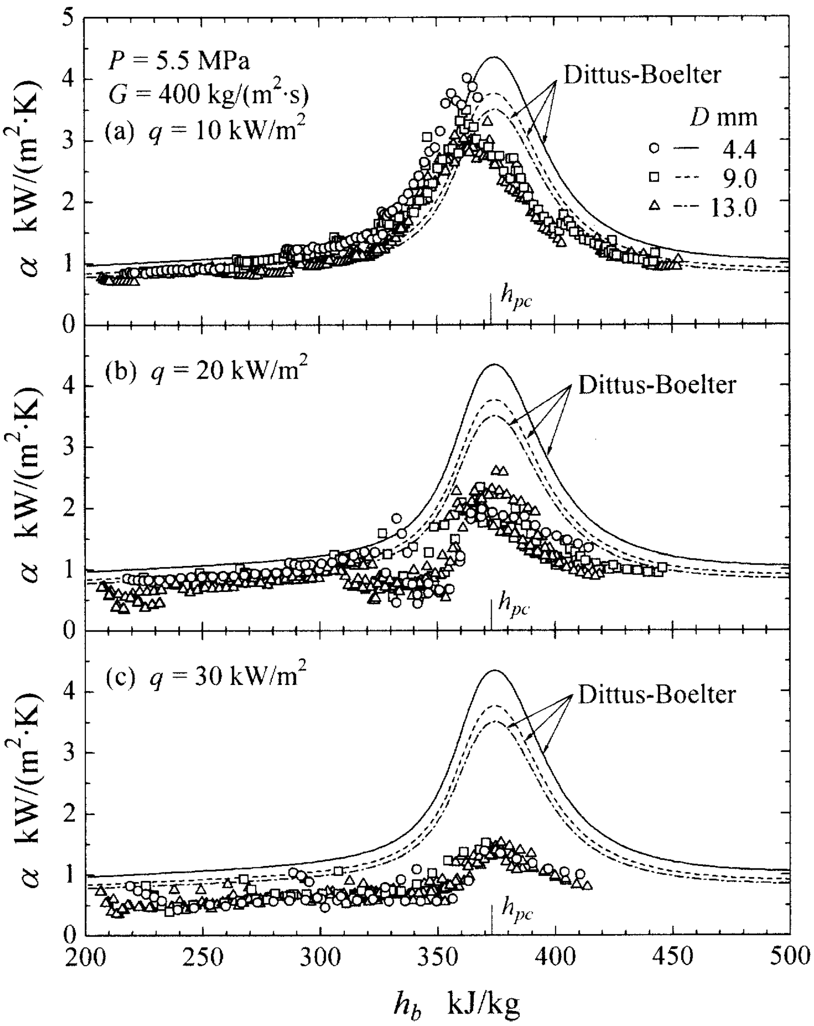


**Fig. 6** Effect of tube diameter on heat transfer coefficient

decreasing the tube diameter is the same as that by the Dittus and Boelter correlation.

In **Figs. 6(b) and 6(c)**, however, the noticeable effect of the tube diameter was not recognized in the region of the 'deteriorated' heat transfer. Therefore, the reduction in the heat transfer coefficient due to the occurrence of the deterioration is more significant for the smaller diameter tube.

For the limit heat flux above which the deterioration in heat transfer occurs, there was found a certain difference among the differnt diameter tubes. **Figure 7** shows the relation between the limit heat flux $q_{lim}$ and the bulk fluid enthalpy $h_b$ with the tube diameter $D$ as a parameter. The limit heat flux generally decreases as the bulk fluid enthalpy increases. It is larger for the smaller diameter tube, although the difference in the limit heat flux becomes small near the pseudocritical point. This improvement in the limit heat flux for the smaller diameter tube is considered due to the better heat transfer in the 'normal' heat transfer, as shown in **Fig. 6**.

### 3.1.3 Predicting performance of 'normal' heat transfer

For the 'normal' heat transfer, various correlations taking account of the effect of the variation of physical properties with temperature have been developed based on the experimental data of water and/or carbon dioxide. Most of these correlations are expressed in

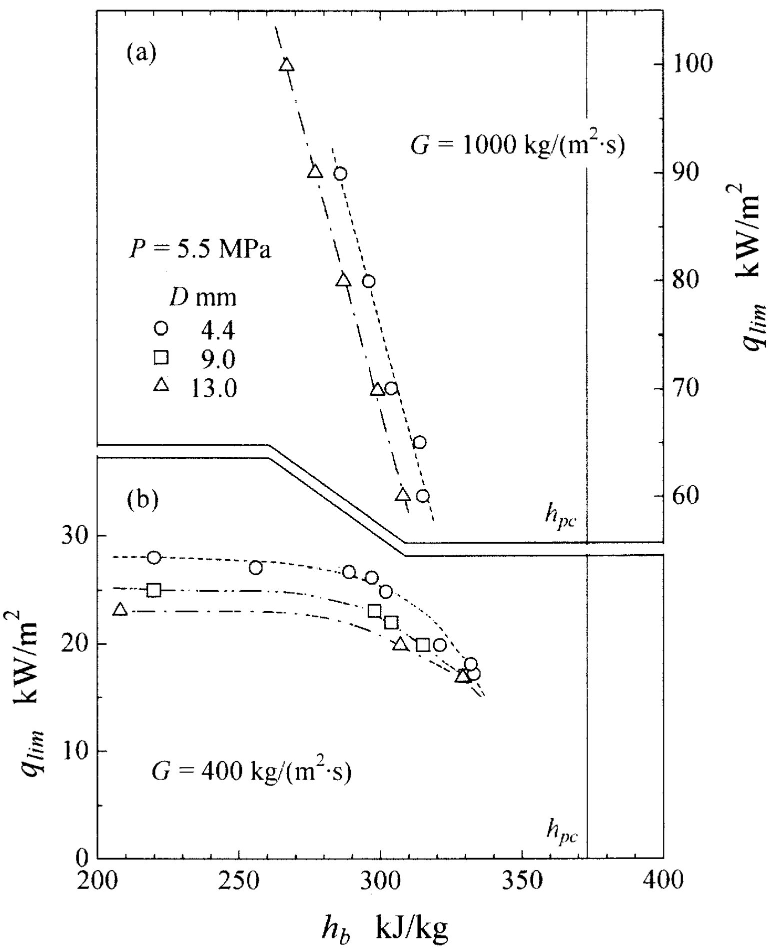


**Fig. 7** Effect of tube diameter on limit heat flux

the form of a constant properties heat transfer correlation equation multiplied by the ratios of properties between the bulk fluid temperature and the wall temperature. Jackson and Hall[7] discussed about the predicting performance of these correlations using approximately 2000 experimental data for water and carbon dioxide, and concluded that the correlation proposed by Krasnoshchekov and Protopopov[16] showed the best predicting performance. In addition, Jackson and Hall proposed a modified form of the Krasnoshchekov and Protopopov correlation and also a simplified form of the modified Krasnoshchekov and Protopopov correlation, although this simplification was originally made by Jackson and Fewster[7]. These two correlations also showed the satisfactorily good predicting performance for the 'normal' heat transfer. After the study by Jackson and Hall, new 'normal' heat transfer correlations have been proposed by Watts and Chou[17] and by Kurganov[18]. In this section, the predicting performance of the various correlations was tested comparing with the present data for the small diameter tube.

In the comparison, the measured heat transfer coefficient data over 1300 were divided with the bulk fluid enthalpy into two groups; the near-pseudocritical region where the property variations are large and the other region approximately treated as a constant property fluid. Here, the near-pseudocritical region is conveniently defined as the region in which the fluid Prandtl number exceeds the value of the fully constant physical properties region by 10% of the difference between the value in the constant properties region and the peak value near the pseudocritical point. For HCFC22 at 5.5 MPa, the near-pseudocritical region corresponds to the range of the fluid enthalpy from 330 to 420 kJ/kg.

The results of the comparison are shown in **Table 2**. In the table, *SD*, *MD* and *AD* are standard deviation, mean deviation and average deviation, respectively, defined by following equations.

$$SD=\sqrt{\frac{1}{N}\sum\left(\frac{\alpha_{cal}-\alpha_{exp}}{\alpha_{exp}}\right)^2} \tag{2}$$

$$MD=\frac{1}{N}\sum\left|\frac{\alpha_{cal}-\alpha_{exp}}{\alpha_{exp}}\right| \tag{3}$$

$$AD=\frac{1}{N}\sum\left(\frac{\alpha_{cal}-\alpha_{exp}}{\alpha_{exp}}\right) \tag{4}$$

The rows of ±10%, ±20% and ±30% express the ratios of the number of the data of its prediction deviation within ±10%, ±20% and ±30% to the total experimental data, respectively.

**Table 2** Predicting performance of the correlations for the 'normal' heat transfer

| Correlations | Krasnoshchekov and Protopopov[16] | Modified Krasnoshchekov and Protopopov[7] | Jackson and Fewster[7] | Watts and Chou[17] | Kurganov[18] |
|---|---|---|---|---|---|
| Constant property region [Number of data=867] | | | | | |
| *SD* | 18.5 | 19.4 | 21.8 | 18.3 | 30.6 |
| *MD* | 16.9 | 18.1 | 20.4 | 16.8 | 28.3 |
| *AD* | 16.8 | 18.0 | 20.3 | 16.6 | 28.3 |
| ±10% | 14.5 | 11.0 | 8.3 | 15.4 | 5.2 |
| ±20% | 69.3 | 58.7 | 43.9 | 70.2 | 18.2 |
| ±30% | 95.4 | 94.9 | 91.3 | 95.4 | 61.9 |
| Near-pseudocritical region [Number of data=465] | | | | | |
| *SD* | 32.4 | 35.9 | 27.8 | 18.3 | 42.7 |
| *MD* | 26.3 | 29.8 | 24.6 | 15.0 | 36.1 |
| *AD* | 25.4 | 29.4 | 24.4 | 14.4 | 36.0 |
| ±10% | 21.7 | 16.6 | 13.5 | 36.2 | 11.4 |
| ±20% | 46.5 | 39.7 | 35.9 | 70.6 | 27.5 |
| ±30% | 63.8 | 55.1 | 67.8 | 92.0 | 47.4 |
| Total [Number of data=1332] | | | | | |
| *SD* | 24.3 | 26.4 | 24.0 | 18.3 | 35.3 |
| *MD* | 20.2 | 22.2 | 21.9 | 16.2 | 31.0 |
| *AD* | 19.8 | 22.0 | 21.7 | 15.9 | 31.0 |
| ±10% | 17.0 | 13.0 | 10.1 | 22.7 | 7.3 |
| ±20% | 61.3 | 52.1 | 41.1 | 70.3 | 21.4 |
| ±30% | 84.4 | 81.0 | 83.1 | 94.2 | 56.8 |

It can be clearly seen in **Table 2** that the Watts and Chou correlation[17)] is superior to other correlations in the near-pseudocritical region, although all correlations except for the Kurganov correlation fit well to the experimental data in the constant property region. Therefore, the Watts and Chou correlation is the most applicable to the tube of small diameter.

**Figures** 8 **and** 9 show the examples of the comparison of various correlations with the experimental data at low and high mass velocities, respectively, in the relation between the heat transfer coefficient $\alpha$ and the bulk fluid enthalpy $h_b$. The prediction by the Dittus and Boelter correlation are also shown in the figures. The Watts and Chou correlation shows good predictions, especially in the near-pseudocritical region including the peak of the heat transfer coefficient at both mass velocities.

Furthermore, **Figs. 10 and 11** show the examples of the comparison of the various

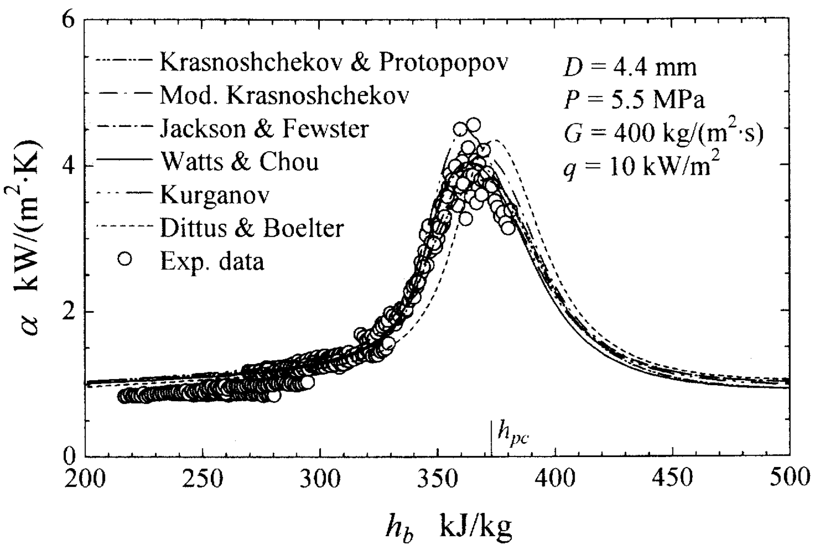


**Fig.** 8 Comparison of the correlations with the present data for the 'normal' heat transfer

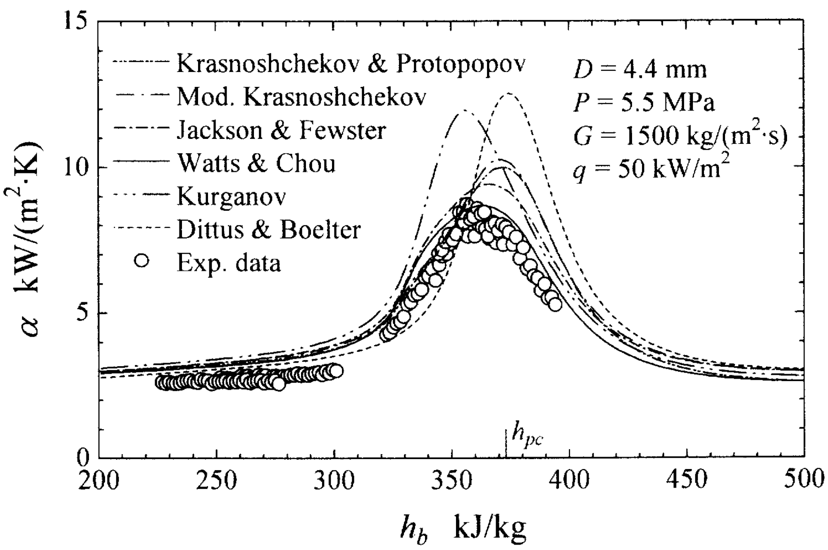


**Fig.** 9 Comparison of the correlations with the present data for the 'normal' heat transfer

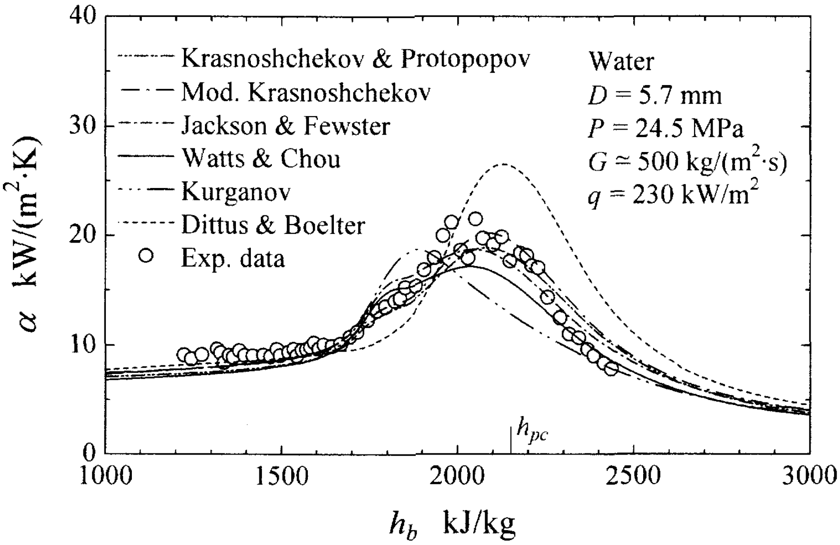


**Fig. 10** Comparison of the correlations with the data for water

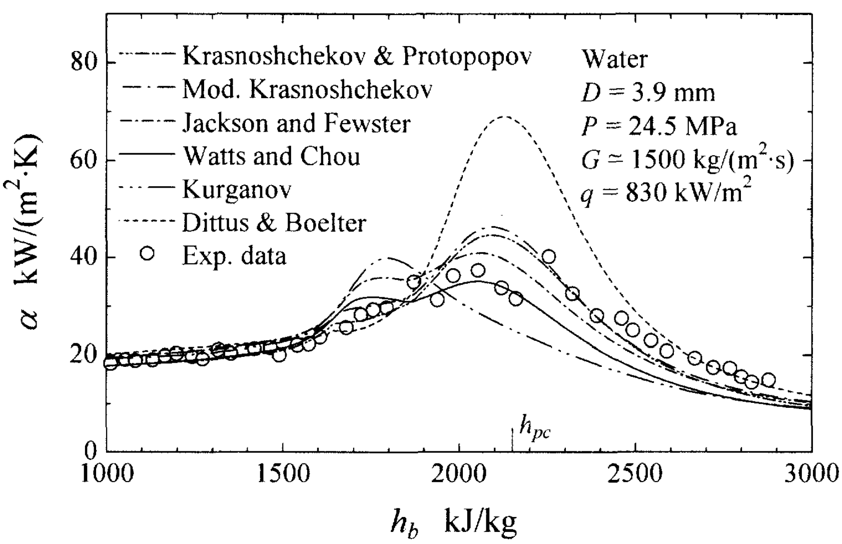


**Fig. 11** Comparison of the correlations with the data for water

correlations with the 'normal' heat transfer data for water obtained with the tubes of small diameter 3.9 and 5.7 mm[13]. The Watts and Chou correlation shows the satisfactorily good predictions for water.

From these results, the Watts and Chou correlation is the most effective in the prediction of the 'normal' heat transfer for the small diameter tube.

### 3.2 Characteristics of Pressure Drop

The frictional pressure drop over the heated test section $\Delta P_f$ was evaluated by subtracting the static pressure drop $\Delta P_h$ and the accelerational pressure drop $\Delta P_a$ from the total pressure drop over the heated section $\Delta P_t$:

$$\Delta P_f = \Delta P_t - \Delta P_h - \Delta P_a \qquad (5)$$

where the total pressure drop $\Delta P_t$ was determined from the pressure difference measured with the differential pressure transmitter, taking account of the static pressure drop in the lead-out pipes connecting pressure taps fixed in the test section and the transmitter and of the pressure drops in the non-heated sections between pressure taps and the heated section. In the calculation of the static pressure drop $\Delta P_h$ and accelerational pressure drop $\Delta P_a$ over the heating section, the axial variation of the fluid density through the heated section was taken into account.

The obtained frictional pressure drops $\Delta P_f$ are plotted against the bulk fluid enthalpy $h_b$ in the lower diagram of **Fig. 12**, with the heat flux $q$ as a parameter. The data for an isothermal flow ($q$=0 kW/m$^2$) are also plotted. The bulk fluid enthalpy for each datum point expresses the mean bulk fluid enthalpy over the heated section. The bar added to the each symbol indicates the estimation error range. Solid symbols denote the data points that involve the 'deteriorated' heat transfer in a certain portion of the heated section. The distribution of the measured inside surface wall temperature $T_w$ for each datum point is plotted in the upper diagram of **Fig. 12**, except for the isothermal flow. In the upper diagram solid symbols denote the axially first measuring positions for the data obtained at different inlet enthalpies.

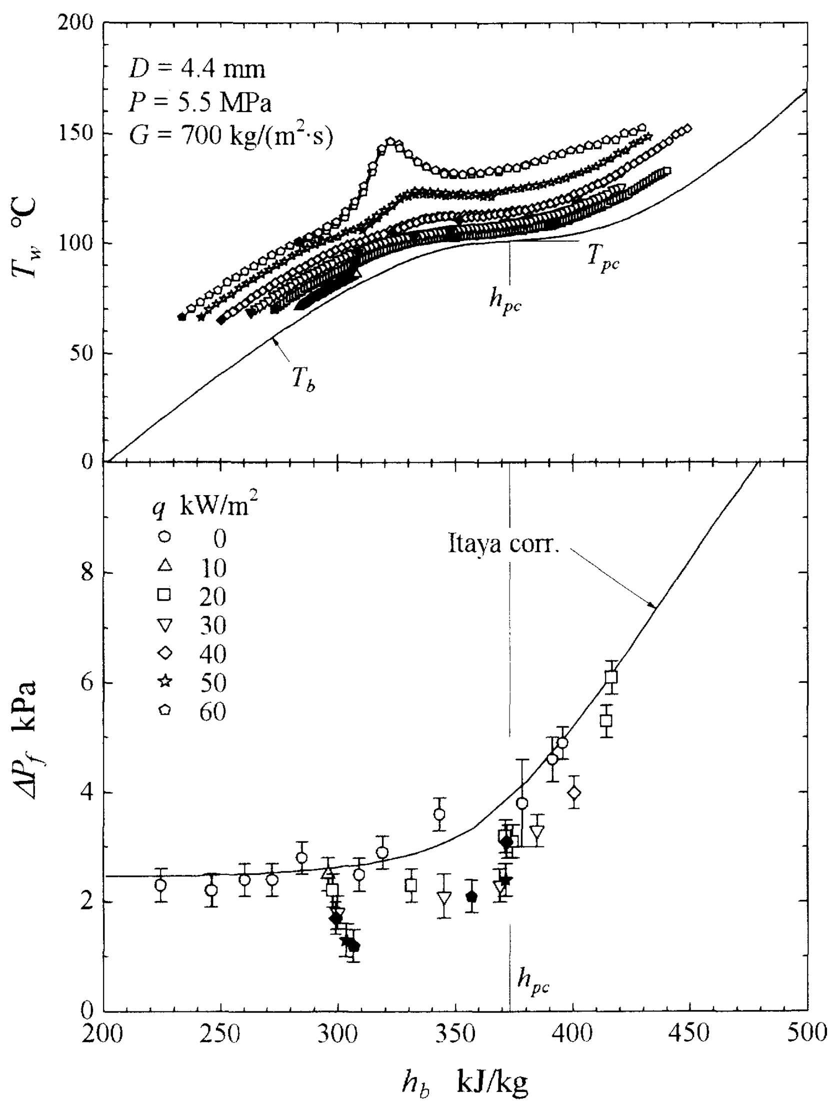


**Fig. 12** Relation of frictional pressure drop and bulk fluid enthalpy

For the isothermal flow, the measured frictional pressure drops showed the good agreement with those calculated using the Itaya correlation for isothermal single phase flow[19]:

$$\xi_0=\frac{0.314}{0.7-1.65\log Re_b+(\log Re_b)^2} \tag{6}$$

where $\xi_0$ is a friction factor for isothermal flow and $Re_b$ is the Reynolds number.

It can be seen that when the fluid is heated ($q\neq0$ kW/m$^2$), the frictional pressure drop $\Delta P_f$ falls down from the value for the isothermal flow in the region near the pseudocritical point, and that this reduction becomes more remarkable with increase in heat flux. These characteristics are similar to those observed by Ishigai *et al.* for water[11]. The low frictional pressure drop at high heat flux in the near-pseudocritical region is attributed mainly to the viscosity reduction of the fluid close to the tube wall due to the high wall temperature.

In the present study, to clarify the relation between the frictional pressure drop and the heat transfer, the frictional pressure drop was examined separately for the 'normal' heat transfer and the 'deteriorated' heat transfer. Such consideration has not been made so far. Here, first the correlation of the friction factor was obtained for the 'normal' heat transfer based on the present data, and then the frictional pressure drop only in the portion of the 'deteriorated' heat transfer was examined.

The friction factor correlation for the 'normal' heat transfer was developed in the following way. For all the data showing the 'normal' heat transfer over the entire heated section, the mean friction factor $\xi_m$ over the heated section was calculated from the measured frictional pressure drop $\Delta P_f$ with the following equation:

$$\xi_m=\Delta P_f\frac{2\rho_m}{G^2}\frac{D}{L_h} \tag{7}$$

where $L_h$ is the length of the heated section and $\rho_m$ is the mean fluid density over the heated section as:

$$\rho_m=\frac{1}{L_h}\int_0^{L_h}\rho_b\,dL \tag{8}$$

Here, $\rho_b$ is the bulk fluid density and $L$ is the distance from the inlet of the heated section. Based on the obtained friction factor data, the following equation was developed for the friction factor $\xi$ in the 'normal' heat transfer, taking account of sharp change of the fluid viscosity with the temperature in the near-pseudocritical region.

$$\xi=\xi_0\left(\frac{\mu_w}{\mu_b}\right)^{0.72} \tag{9}$$

where $\xi_0$ is the friction factor for the isothermal flow given by the Itaya correlation and $\mu_w/\mu_b$ is the viscosity ratio between the wall temperature and the bulk fluid temperature. This equation correlates the obtained friction factor within the deviation of $\pm15\%$.

With using equation (9), the frictional pressure drop only in the 'deteriorated' heat transfer portion was evaluated for the data involving the 'deteriorated' heat transfer in a certain portion of the heated section, by subtracting the frictional pressure drop in the 'normal' heat transfer portion from the measured total frictional pressure drop over the entire heated section. In this calculation, the frictional pressure drop in the 'normal' heat transfer portion was evaluated from equation (9).

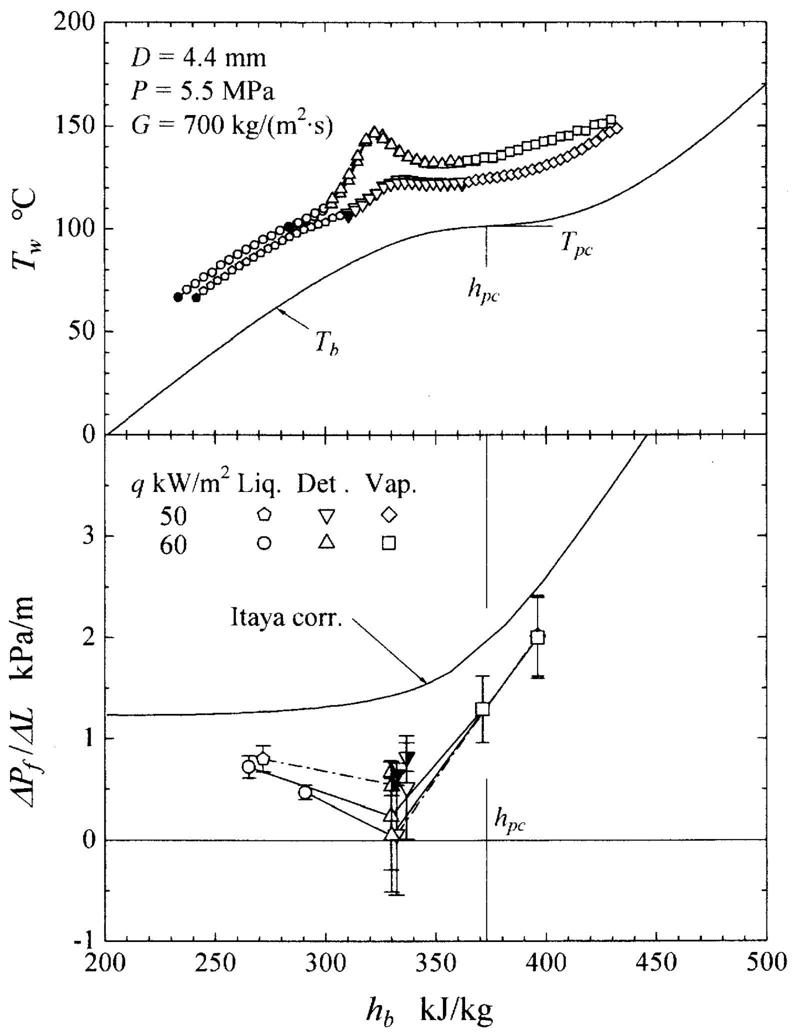


**Fig. 13** Frictional pressure gradient in the 'normal' and 'deteriorated' heat transfer

**Figure 13** shows the results of the evaluated frictional pressure drop only in the 'deteriorated' heat transfer portion. In the upper diagram of **Fig. 13**, the data used for the evaluation are given in the relation of the wall temperature $T_w$ and the bulk fluid enthalpy $h_b$. Solid symbols indicate the axially first measuring positions for the data obtained at different inlet enthalpies. For each data, the datum point in the 'deteriorated' heat transfer portion is denoted by the triangular or inverted-triangular symbol, while the point in the 'normal' heat transfer is by other symbols. The letter "Det." indicates the 'deteriorated' heat transfer portion and the "Liq." and "Vap." express the 'normal' heat transfer portions upstream and downstream of the 'deteriorated' portion, respectively. The evaluated frictional pressure drops over the 'deteriorated' heat transfer portions are shown in the lower diagram of **Fig. 13**, in the form of the frictional pressure gradient $\Delta P_f/\Delta L$, separately from the values for the 'normal' heat transfer portions. Semi-solid symbols for the 'deteriorated' heat transfer portion denote the values calculated by applying equation (9) for the 'normal' heat transfer to the 'deteriorated' portion. The bar added to the each symbol indicates the evaluation error range.

It can be clearly found that, in the portion of the 'deteriorated' heat transfer, the frictional pressure drop is smaller than that calculated value with equation (9) and therefore is much lower than the value for the isothermal flow. This large reduction of the frictional pressure drop is supposed to be affected by the less production of turbulence in the fluid layer near the wall brought about under the 'deteriorated' heat transfer condition described previously.

## 4. Conclusions

In relation to the development of the SCPR, experiments were performed on the heat transfer and pressure drop for supercritical pressure fluid flowing upward in a uniformly heated vertical tube of small diameter 4.4 mm, using HCFC22 as the test fluid. The following results were obtained.

Characteristics of the heat transfer are similar to those in the tubes of large diameter. The effect of tube diameter on the heat transfer was seen for the 'normal' heat transfer, but not for the 'deteriorated' heat transfer. The limit heat flux for the occurrence of deterioration in heat transfer becomes larger for the smaller diameter tube. Among the various correlations for the 'normal' heat transfer, the Watts and Chou correlation shows the best predicting performance.

The frictional pressure drop in the near-pseudocritical region becomes smaller as the heat flux increases. The friction factor correlation for the 'normal' heat transfer was obtained based on the present data. The reduction in the frictional pressure drop was found more remarkable in the portion of the 'deteriorated' heat transfer.

## Acknowledgements

This study was performed as a part of the SCPR development project funded by the Institute of Applied Energy (IAE), Ministry of Economy, Trade and Industry (METI), Japan. The authors wish to thank Messrs. M. Hayano and K. Maruyama for their contribution in obtaining the data presented.

## Nomenclature

| | |
|---|---|
| $c_p$ | specific heat at constant pressure [kJ/(kg·K)] |
| $D$ | tube inside diameter [m] |
| $G$ | mass velocity [kg/(m$^2$·s)] |
| $h$ | specific enthalpy [kJ/kg] |
| $L$ | distance from the inlet of the heated section [m] |
| $L_h$ | heated length of the test section [m] |
| $P$ | pressure [MPa] |
| $\Delta P$ | pressure drop [kPa] |
| $q$ | heat flux [kW/m$^2$] |
| $T$ | temperature [°C] |
| $\alpha$ | heat transfer coefficient [kW/(m$^2$·K)] |
| $\lambda$ | thermal conductivity [kW/(m·K)] |
| $\mu$ | viscosity [Pa·s] |
| $\xi$ | friction factor |
| $\rho$ | density [kg/m$^3$] |

**subscripts**

| | |
|---|---|
| 0 | isothermal |
| $a$ | accelerational |

| | |
|---|---|
| *b* | bulk fluid |
| *cal* | calculated |
| *cr* | critical |
| *exp* | experimental |
| *f* | frictional |
| *h* | static |
| *m* | mean |
| *pc* | pseudocritical |
| *t* | total |
| *w* | wall |

## References

1) Y. Oka and S. Koshizuka, "Design concept of once-through cycle supercritical-pressure light water cooled reactors," Proc. of SCR-2000: The First Int. Symp. on Supercritical Water-cooled Reactors, Design and Technology, 1 (2000).
2) M. A. Styrikowitsch, S. L. Miropolsky and M. E. Schizman, "Wärmeübergang im kritischen Druckgebiet bei erzwungener Strömung," VGB, 61, 288 (1959).
3) H. S. Swenson, J. R. Carver and C. R. Kakarala, "Heat transfer to supercritical water in smooth-bore tubes," Trans. ASME, J. Heat Transfer, 87, 477 (1965).
4) G. Domin, "Heat transfer to water in pipes in the critical/supercritical region," B.W.K., 15 [11], 527 (1963).
5) M. E. Shitsman, "Temperature conditions in tubes at supercritical pressures," Thermal Engineering, 15 [5], 72 (1968).
6) K. Yamagata *et al.*, "Forced convective heat transfer to supercritical water flowing in tubes," Int. J. Heat Mass Transfer, 15 [12], 2575 (1972).
7) J. D. Jackson and W. B. Hall, "Forced convection heat transfer to fluids at supercritical pressure," Turbulent Forced Convection in Channels and Bundles edited by S. Kakaç and D. B. Spalding, Vol.2, Hemisphere Pub., 563 (1979).
8) F. W. Dittus and L. M. K. Boelter, "Heat transfer in automobile radiators of the tubular type," University of California Publications in Engineering, 2, 443 (1930).
9) S. Yoshida, "Heat transfer to freon at high pressures in evaporator-tubes," Reports of Special Project Research on Energy, SPEY23, 39 (1987).
10) S. Yoshida *et al.*, "Criterion for the occurrence of deterioration in heat transfer at a supercritical pressure," Prepr. of JSME, 852-2, (1985), [in Japanese].
11) S. Ishigai *et al.*, "Forced convective heat transfer and pressure drop for supercritical water flowing in tube (2nd report, Experimental results of pressure drop and relation between heat transfer and fluid friction)," Trans. JSME, 47 [424], 2343 (1981), [in Japanese].
12) B. Shiralkar and P. Griffith, "The effect of swirl, inlet conditions, flow direction, and tube diameter on the heat transfer to fluids at supercritical pressure," Journal of Heat Transfer, 92, 465 (1970).
13) S. Ishigai *et al.*, "Forced convective heat transfer and pressure drop for supercritical water flowing in tube (1st report, Experimental results of heat transfer)," Trans. JSME, 47 [424], 2333 (1981), [in Japanese].
14) S. Yoshida, H. Mori and M. Ohno, "Heat transfer to freon in the critical region," Reports of Special Project Research on Energy, SPEY14, 153 (1987).
15) J. Gallagher *et al.*, NIST Standard Reference Data Base 23, REFPROP Ver 6.01, (1998).

16) E. A. Krasnoshchekov and V. S. Protopopov, "Experimental study of heat exchange in carbon dioxide in the supercritical range at high temperature drops," Teplofizika Vysokikh Temperatur, 4 [3], 389 (1966).
17) M. J. Watts and C. T. Chou, "Mixed convection heat transfer to supercritical pressure water," Proc. of 7th Int. Heat Transfer Conf. Munchen, 3, 495 (1982).
18) V. A. Kurganov, "Heat transfer and pressure drop in tubes under supercritical pressure of the coolant. Part 1: Specifics of the thermophysical properties, hydrodynamics, and heat transfer of the liquid. Regimes of normal heat transfer," Thermal Engineering, 45 [3], 177 (1998).
19) S. Itaya, "New experimental formula of the coefficient of pipe friction," J. of JSME, 48 [332], 84 (1945), [in Japanese].